Electronic Supplementary Material (ESI) for New Journal of Chemistry.

Electronic Supplementary Material

A Novel High-sensitive Dual-channel Chemical Sensor for Sequential Recognition of Cu^{2+}/CN^- in Aqueous Media and its Bioimaging Applications on Living Cells

Yong-Qiang Xie[a, c], You-Ming Zhang[a, b, *], Zhao-Hui Li[a], Xiao-Ni Qi[a], Hong Yao[a], Bing-Bing Shi[a], Wen-Juan Qu[a], Tai-Bao Wei[a*] and Qi Lin[a, *]

[a] *Key Laboratory of Eco-Environment-Related Polymer Materials, Ministry of Education of China, Key Laboratory of Polymer Materials of Gansu Province, College of Chemistry and Chemical Engineering, Northwest Normal University, Lanzhou, Gansu, 730070, P. R. China;*

[b] *Gansu Natural Energy Research Institute, Lanzhou, 730046, P. R. China;*

[c] *Experimental & Training Teaching Centers, Gansu University of Chinese Medicine Lanzhou, Gansu, 730000, P. R. China.*

*Corresponding author: Tel: +86-931-7973120;

Email: zhangnwnu@126.com(You-Ming Zhang); weitaobao@126.com (Tai-Bao Wei); *linqi2004@126.com (Qi Lin)*

Contents

1. Absorbance spectra of **DH** with increasing concentrations of Cu^{2+}

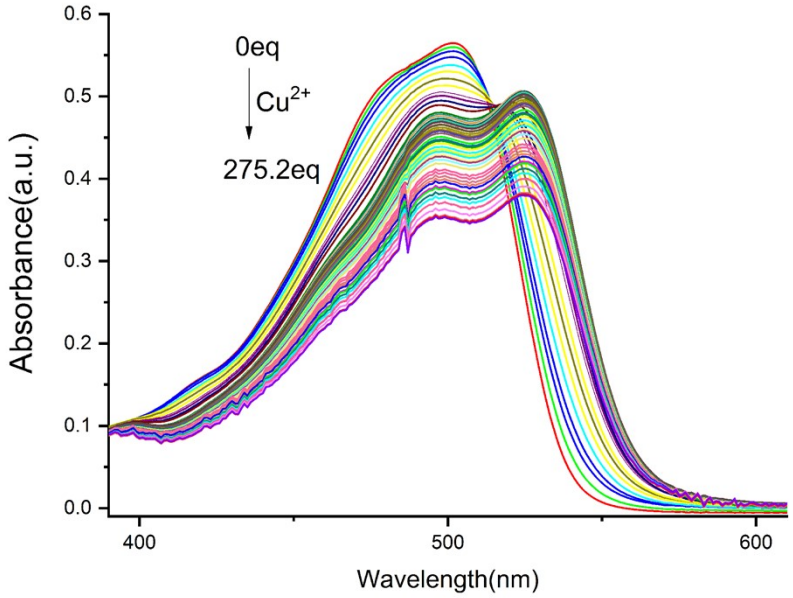

Fig. S1 Absorbance spectra of **DH** (2.0×10^{-5} M) with increasing concentrations of Cu^{2+}, in DMSO/H2O (9 1, v/v) solutions at room temperature.

2. The UV-vis detection limit of Cu^{2+} determined by **DH**

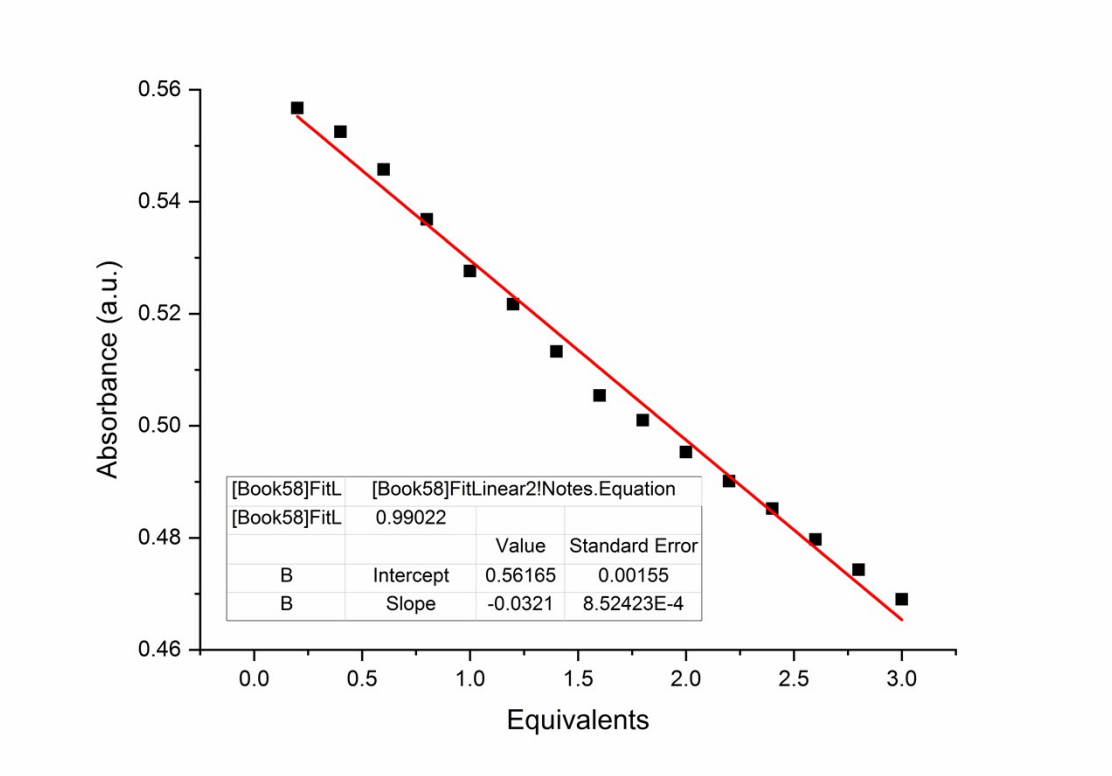

Linear Equation: Y = - 0.0321 × X + 0.56165 R = 0.9902

$S = 3.21 \times 10^4$ $\delta = \sqrt{\frac{\Sigma(A-\bar{A})2}{(N-1)}} =$ 2.884×10^{-2} (N = 15) K = 3

LOD = K × δ/S = 2.7105×10^{-6} M

Fig. S2 The photograph of the UV-vis absorption spectral linear range for Cu^{2+}.

3. The fluorescent detection limit of Cu^{2+} determined by **DH**

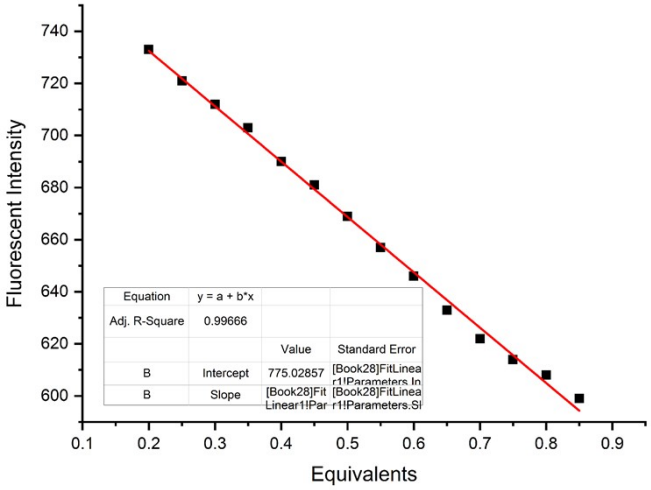

Linear Equation: Y = -212. 5714× X + 775.02857 R = 0.9966

S = 2.225×10^8 $\delta = \sqrt{\frac{\Sigma(F-\bar{F})2}{(N-1)}} =$ 49.93 (N = 15) K = 3

LOD = K × δ/S = 7.048×10^{-7} M

Fig. S3 The photograph of the fluorescent spectrum linear range for Cu^{2+}.

4. Effect of pH on the sensing properties of **DH**

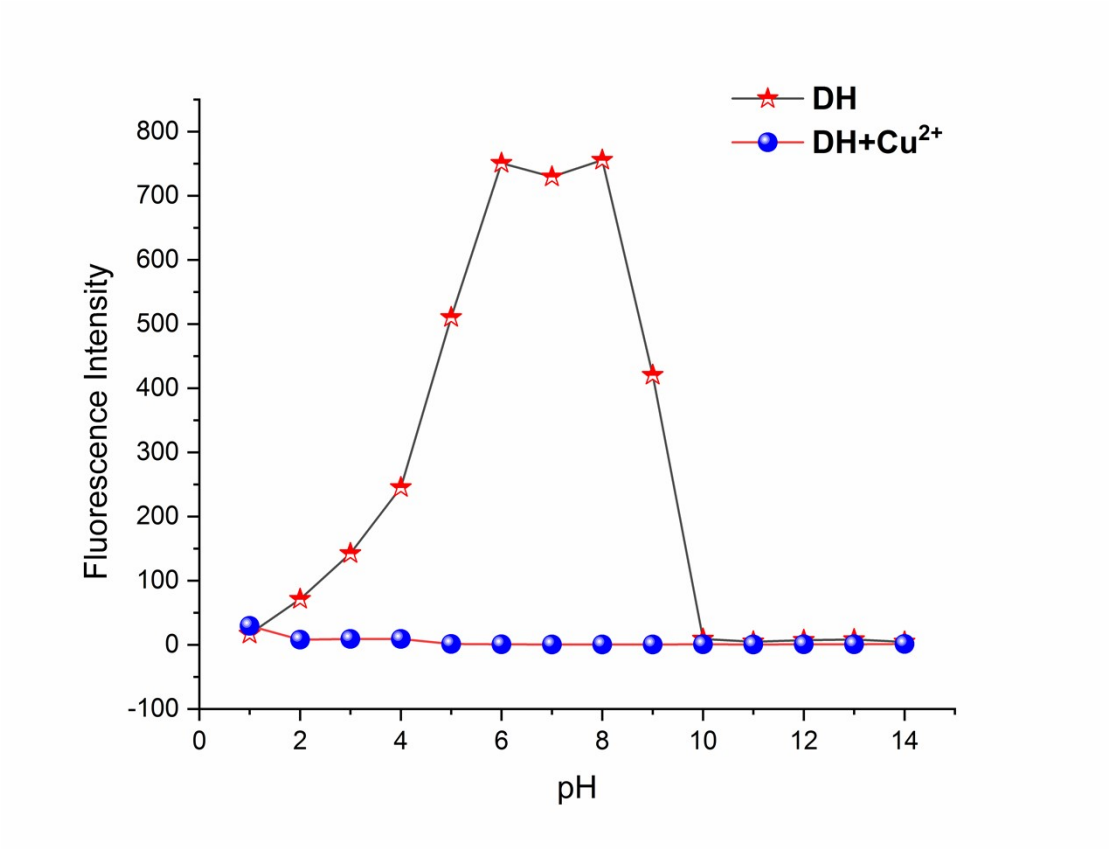

Fig. S4 Effect of pH on the sensing properties of DH in the absence and presence of Cu^{2+}

5. Effect of response time on the fluorescence intensity of **DH-Cu^{2+}**

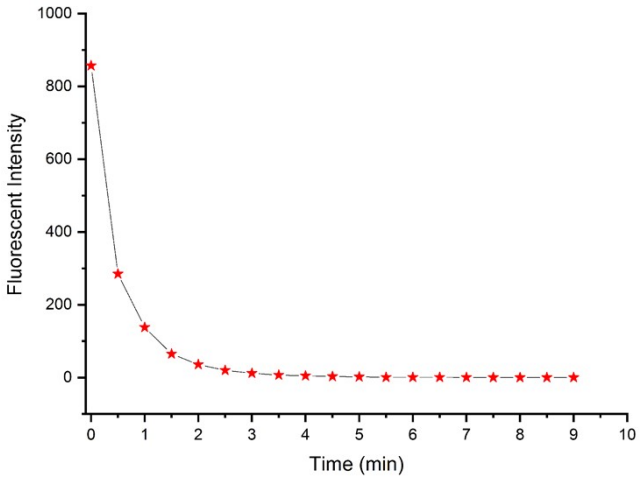

Fig. S5 Effect of response time on the fluorescence intensity of **DH-Cu^{2+}**

6. The fluorescent detection limit of CN^-determined by **DH+ Cu^{2+}**

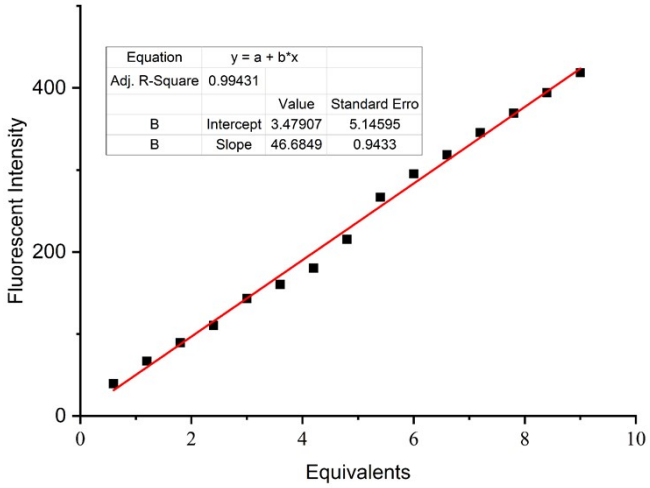

Linear Equation: Y = 46.685 × X + 3.47907 R = 0.99431

$$S = 4.6685\times 10^{7} \quad \delta = \sqrt{\frac{\Sigma(F-\bar{F})2}{(N-1)}} = 0.0420 \quad (N = 15) \quad K = 3$$

$LOD = K \times \delta/S = 8.1067\times10^{-6}$ M

Fig. S6 The photograph of the fluorescent spectrum linear range for CN^-.

7. Fluorescence spectra of **DH** with increasing concentrations of CN^-

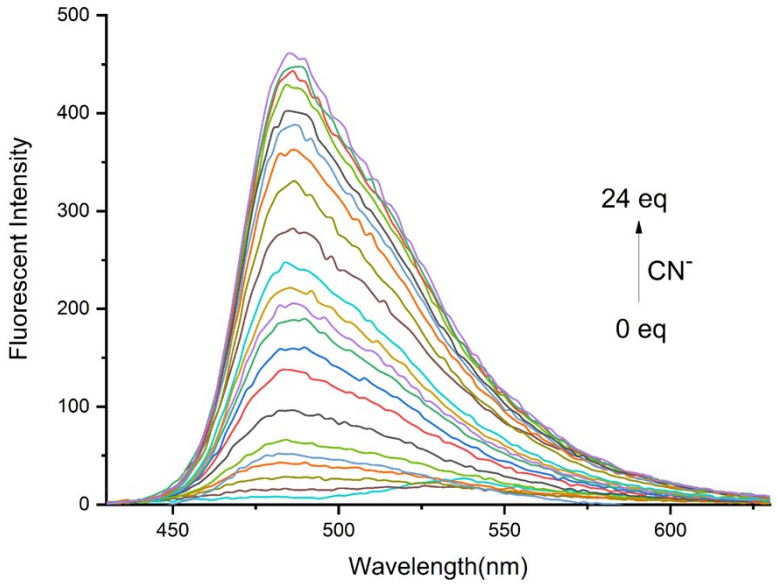

Fig.S7 Fluorescence spectra of **DH** (2.0×10^{-5}) with increasing concentrations of CN^-, in DMSO/H_2O (9 1, v/v) solutions at room temperature (λ_{ex}=415 nm).

8. The fluorescent detection limit of CN^-determined by **DH**

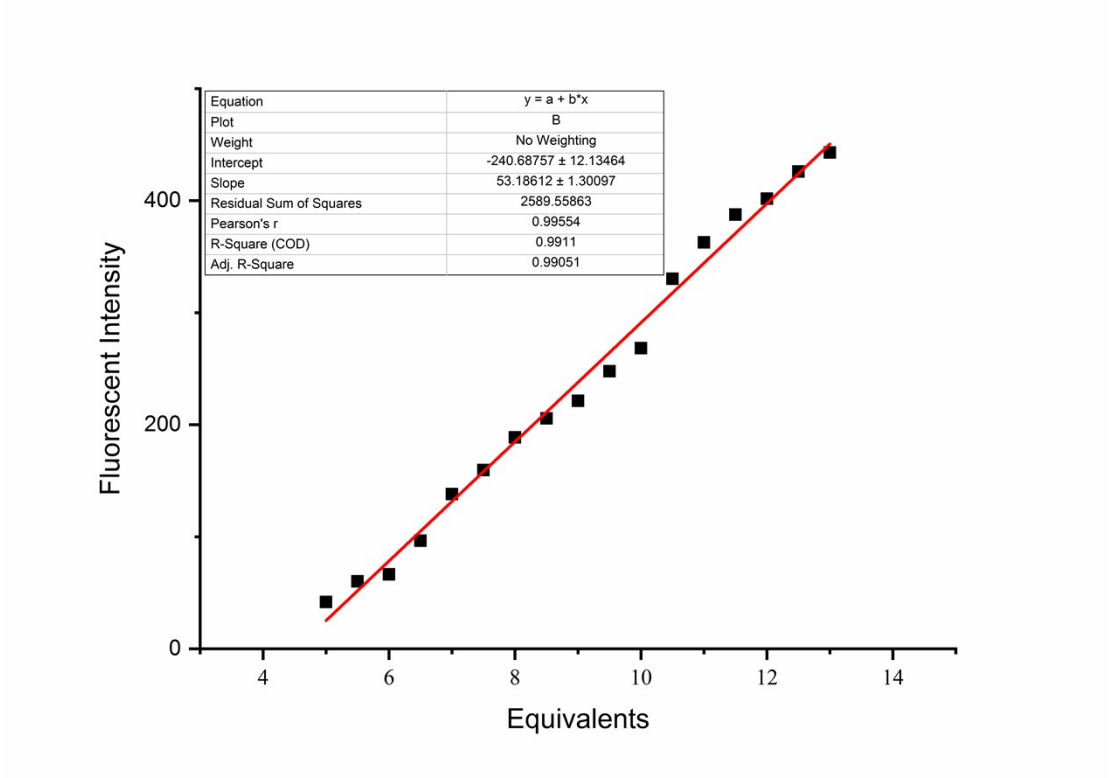

Linear Equation: Y =53.1861 × X + 240.6876 R = 0.99051

S = 5.3186× 10^7 $\delta = \sqrt{\frac{\Sigma(F-\bar{F})2}{(N-1)}} =$ 134.8896 (N = 17) K = 3

LOD = K × δ/S = 7.6085×10^{-6} M

Fig. S8 The photograph of the fluorescent spectrum linear range for CN^-.

9. The Job's plot examined between Cu^{2+} and **DH**

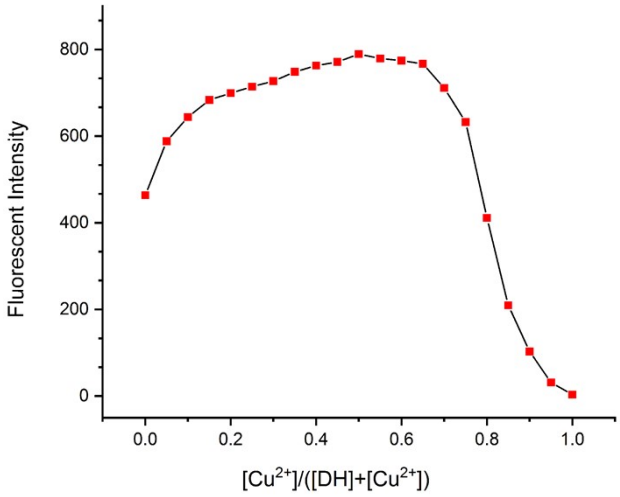

Fig. S9 The Job's plot examined between Cu^{2+} and **DH**, indicating the 1∶2 stoichiometry for **DH** and Cu^{2+}.

10. FT-IR spectra of sensor **DH**, **DH- Cu^{2+}** and **DH- Cu^{2+}-CN^-**

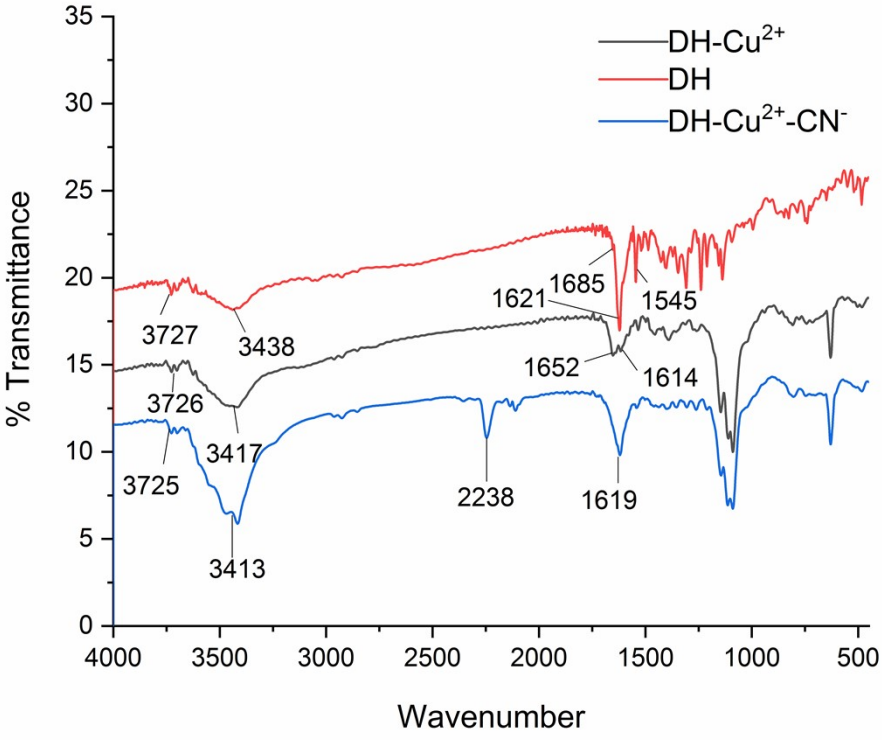

Fig. S10 FT-IR spectra of sensor DH, DH- Cu^{2+} and **DH- Cu^{2+}-CN^-**.

11.ESI/MS of sensor **DH** and after adding Cu^{2+} ions

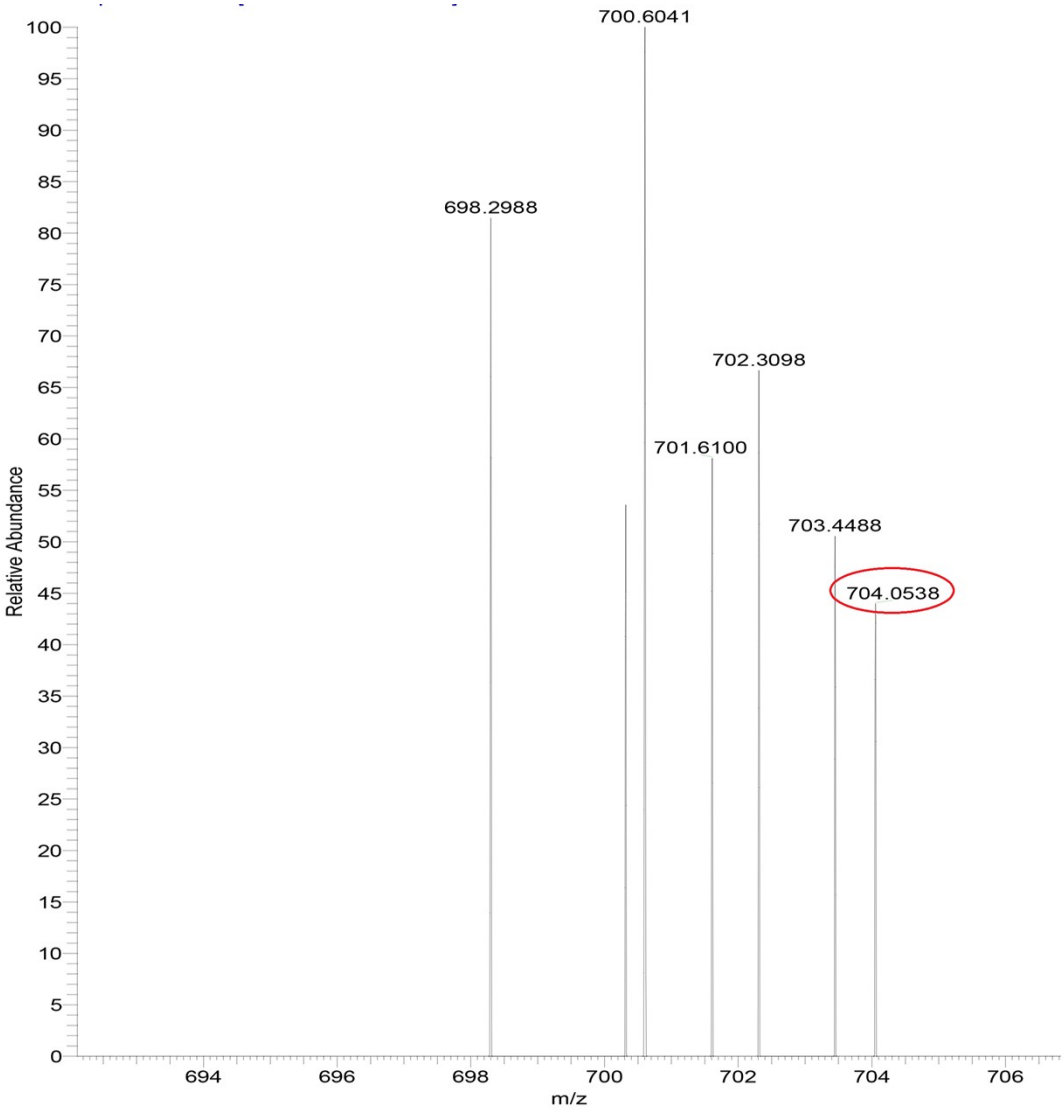

Fig. S11 ESI/MS of sensor **DH** and after adding Cu^{2+}.

12.ESI/MS of **DH–Cu^{2+}** after adding CN^-

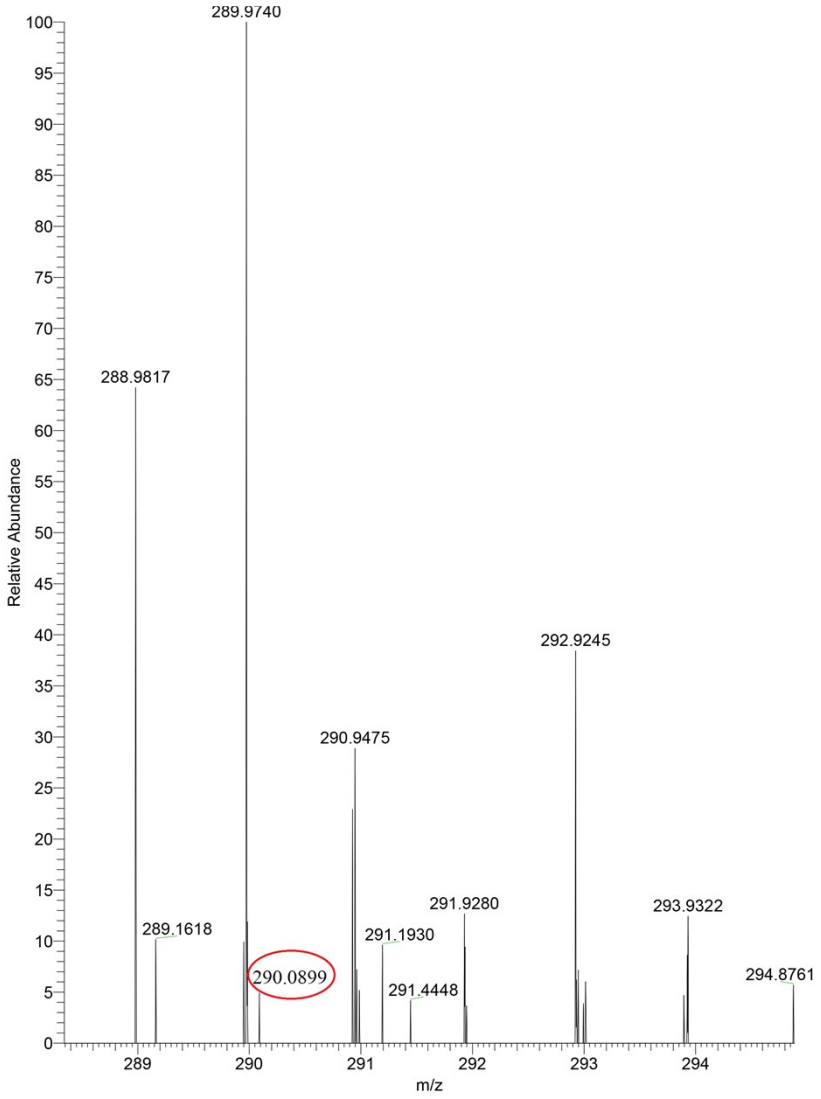

Fig. S12 ESI/MS of **DH-Cu^{2+}** after adding CN^-.

13. ^{1}H–NMR spectrum of **DH**

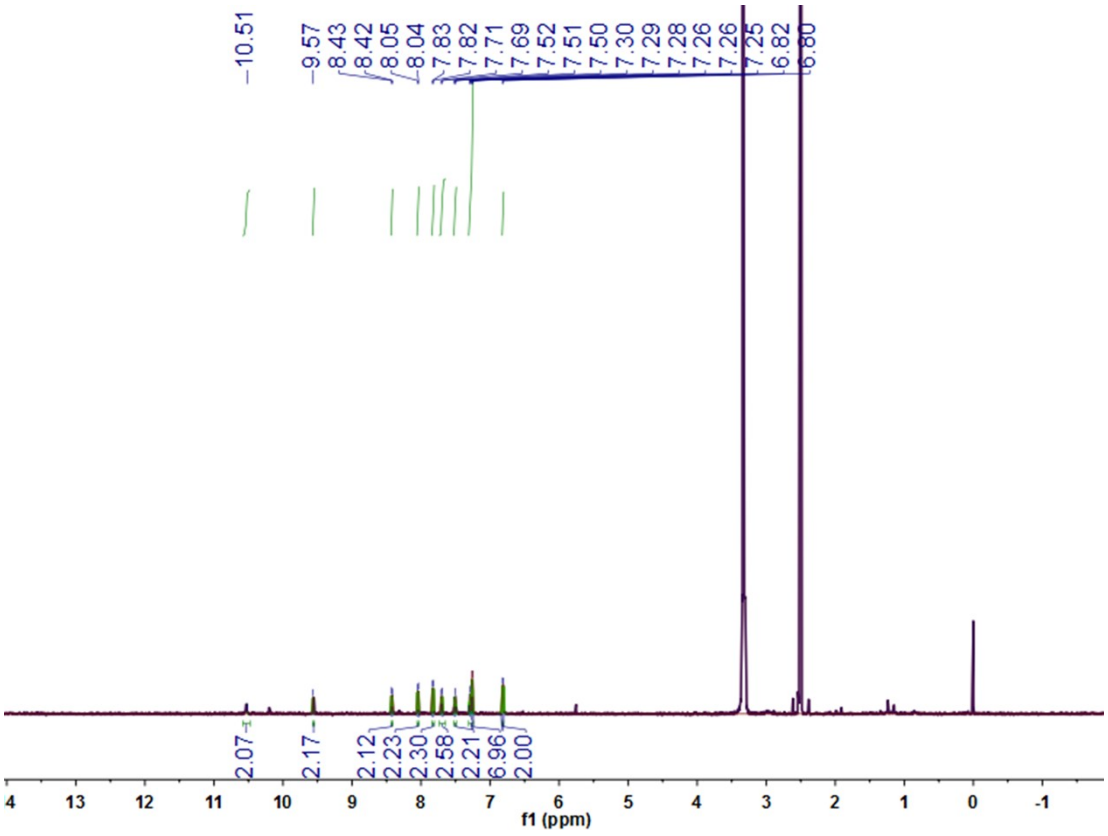

Fig. S13 ^{1}H–NMR spectrum of **DH** in DMSO–d_6.

14. The simulated absorption spectrum of the probe molecules **DH** and **DH-Cu^{2+}** and the absorption spectrum obtained from experiments

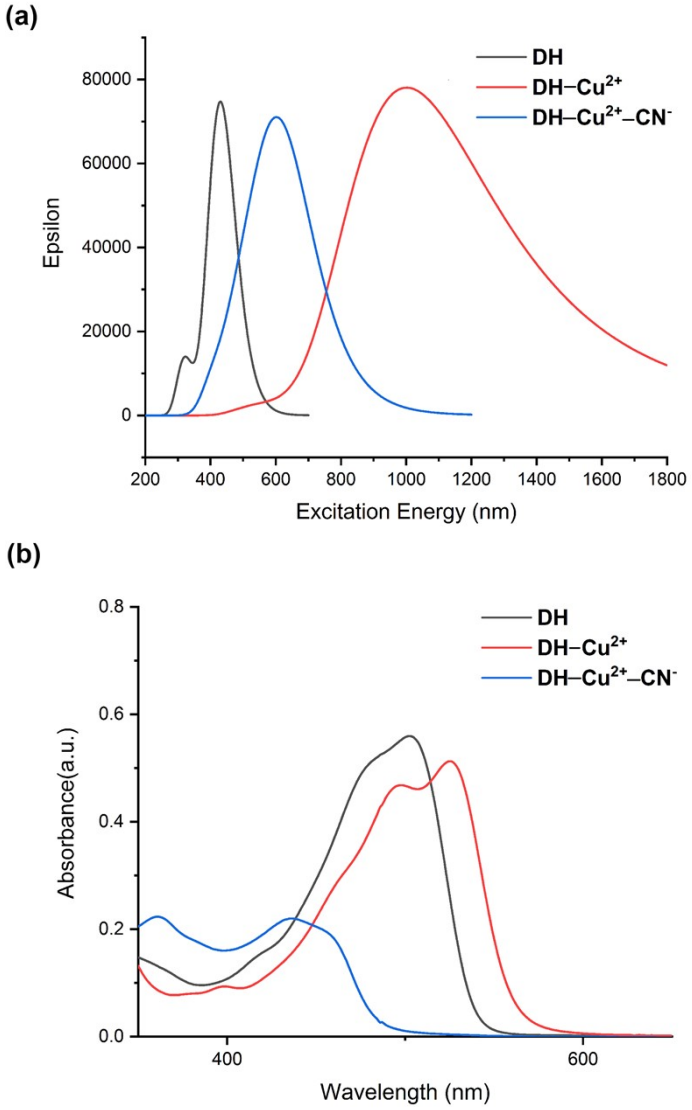

Fig. S14 The simulated absorption spectrum of the probe molecules **DH** and **DH- Cu^{2+}** and the absorption spectrum obtained from experiments.

15. The simulated emission spectrum of the probe molecules **DH**, **DH-Cu^{2+}**, **DH- Cu^{2+}-CN^-** and the emission spectrum obtained from experiments

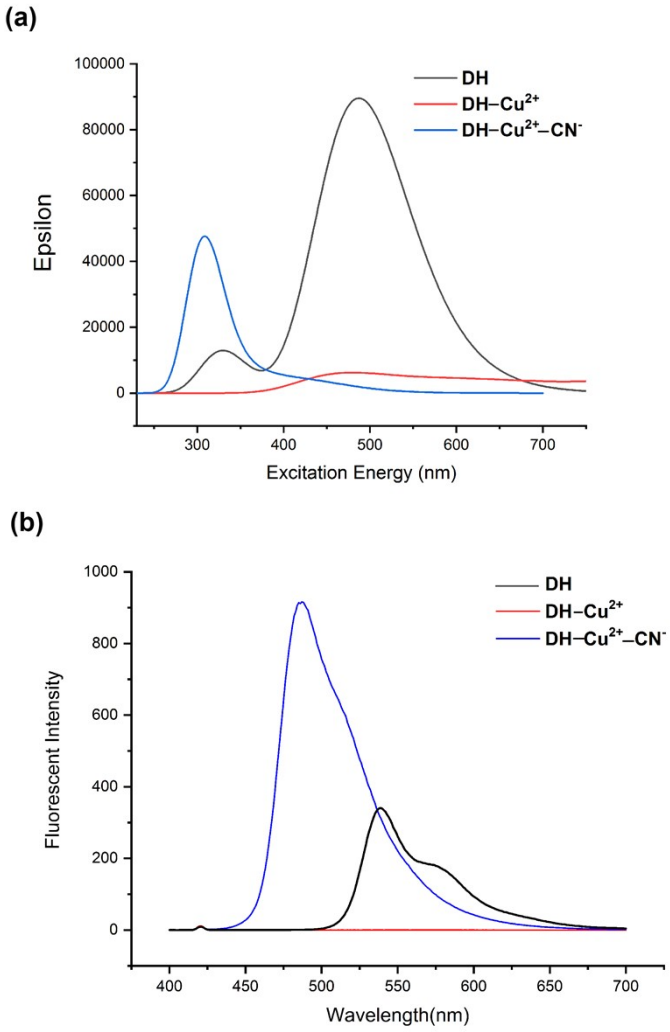

Fig. S15 the simulated emission spectrum of the probe molecules **DH, DH- Cu^{2+}, DH- Cu^{2+}-CN** and the emission spectrum obtained from experiments.

16. Reversible switching cycles of fluorescence intensity by alternate addition of Cu^{2+} and EDTA

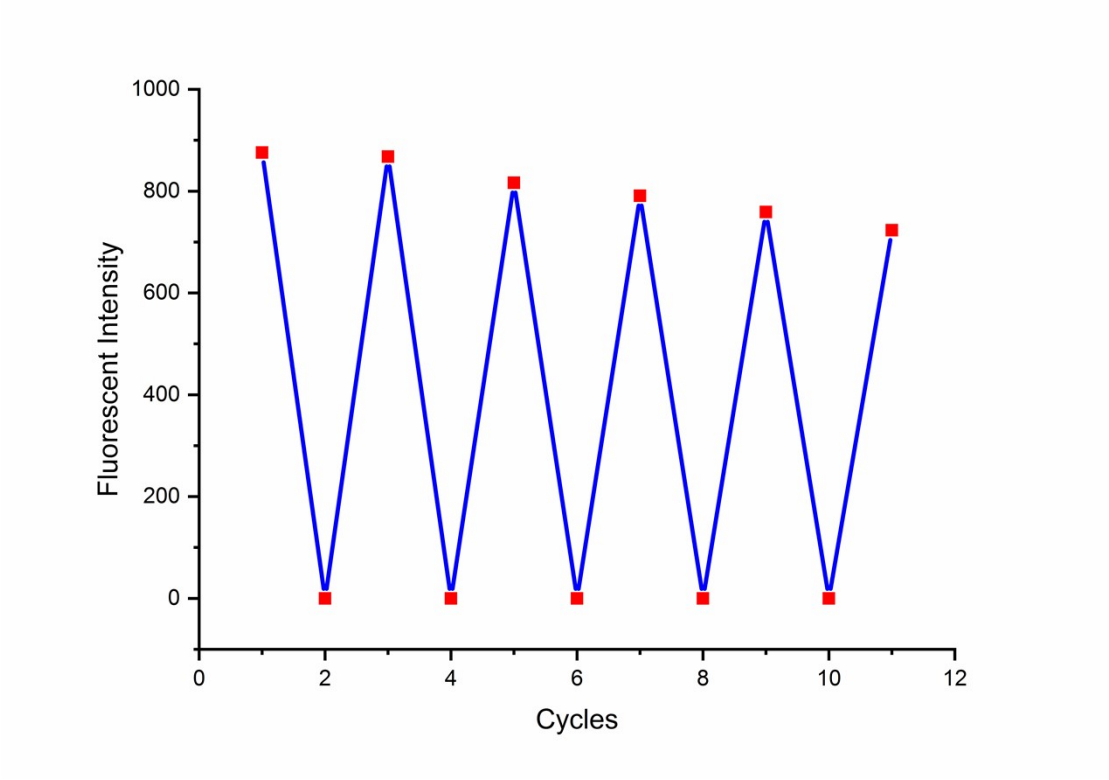

Fig. S16 Reversible switching cycles of fluorescence intensity by alternate addition of Cu^{2+} and EDTA in DMSO/H_2O (**9:1, v/v**) solution (λ_{ex} = 515 nm).

17. Cytotoxicity test of sensor **DH**

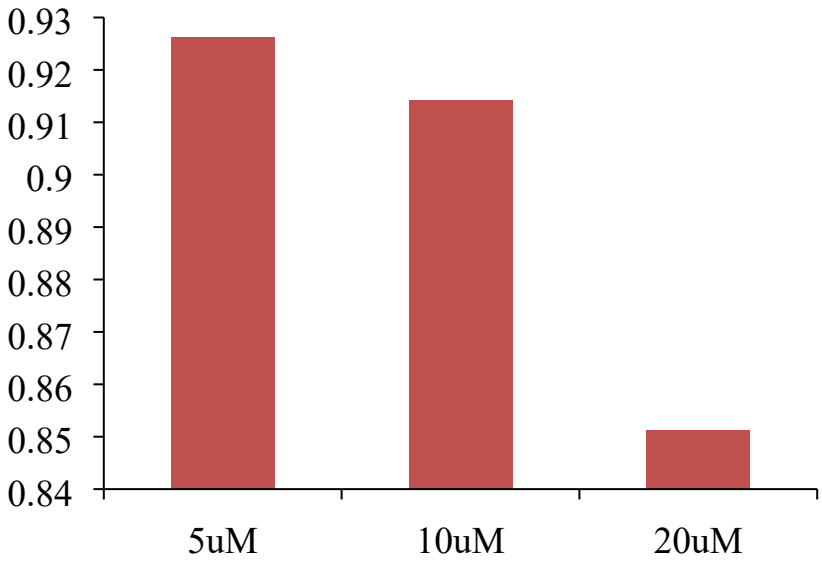

Fig. S17 Cytotoxicity test of sensor **DH**.